Appl. Phys. B 73, 311–316 (2001)
DOI: 10.1007/s003400100653

Applied Physics B
Lasers and Optics

S. LINDEN[1,✉]
A. CHRIST[1]
J. KUHL[1]
H. GIESSEN[2]

Selective suppression of extinction within the plasmon resonance of gold nanoparticles

[1] Max-Planck-Institut für Festkörperforschung, Heisenbergstr. 1, 70569 Stuttgart, Germany
[2] Institute of Applied Physics, University of Bonn, 53115 Bonn, Germany

Received: 3 July 2001
Published online: 10 October 2001 • **© Springer-Verlag 2001**

ABSTRACT We present extinction measurements on rectangular two-dimensional arrays of gold nanoparticles on a dielectric waveguide. The spectra exhibit spectrally narrow bands of suppressed extinction within the particle–plasmon resonance, resulting from destructive interference between the incident light field and the excited waveguide modes. The dependence of the spectral position of these high-transmission bands on different waveguide modes is investigated in detail.

PACS 78.66.-w; 73.20.Mf; 61.46.+w

The extinction spectrum of noble-metal nanoparticles in the visible is governed by resonantly excited electron–plasma oscillations (particle plasmons) [1]. For an isolated spherical particle, the linear optical properties are well described by the Mie theory [2]. In general, the characteristics of the resonance such as center frequency, bandwidth, amplitude, and line shape are determined by several factors: the material, the size, and the shape of the particle, as well as the dielectric function of the surrounding medium. Therefore it is possible within certain limits to 'design' the extinction spectrum accordingly by controlling these parameters. Besides the interesting linear optical features, particle plasmons are distinguished by their ability to generate strong local field enhancement [3] and optical non-linearities [4]. These features account for metal nanoparticles being a promising candidate for future electronic and optical applications.

Modern electron-beam lithographic methods allow us to create regular patterns of metal nanoparticles [5, 6], where the shape and the arrangement of the particles can be matched according to the experimental needs. With these samples it is possible to investigate in detail the influence of the electromagnetic particle–particle interaction on the plasmon resonance. Lamprecht et al. [7] have demonstrated a strong dependence of the resonance width and spectral position on the grating constant in regular two-dimensional patterns of gold nanoparticles. The particles were deposited on top of a quartz substrate covered with a thin (3 nm) indium–tin-oxide (ITO) film. Their findings can be explained by in-phase addition (constructive interference) of the scattered light fields of neighboring particles.

Very recently, we have shown in a series of optical transmission experiments (for experimental details see Fig. 1a) that the regular arrangement of gold nanoparticles on a thick (140 nm) ITO film leads to qualitatively different results [8]. The extinction spectra of these samples exhibit pairs of narrow bands with suppressed extinction within the particle–plasmon resonance (see Fig. 1b, solid line). These bands can be shifted by changing the periodicity of the particles or by varying the angle of incidence. The crucial features of these samples responsible for this effect are the regular arrangement of the nanoparticles and the presence of the thick ITO film below the dots. The thick ITO film is able to support guided modes in the spectral range of the particle plasmons. Due to the chosen regular arrangement of the gold nanoparticles and due to the polarization of the incident light field, a part of this incident light can be coupled into the first transverse electric (TE) waveguide mode. When the excited waveguide mode is resonant to the particle–plasmon resonance, the total electric field acting on the nanoparticles consists of two parts: the incident light and the field of the waveguide mode. The polarizations created by both fields are 180 degrees out of phase [9], which leads to destructive interference between the directly incident radiation and the waveguide mode at the metal-dot positions. As a result, this interference reduces the coupling between the light and the particle plasmons at a spectral position determined by the waveguide mode, which manifests itself as a pronounced dip in the extinction spectrum. The fact that even for normal incidence always two dips appear in the extinction spectra has to be attributed to the formation of two standing waves with nodes between and under the gold nanoparticles. The different dielectric environments of these two waves lift the degeneracy. These new spectral features are not present in the extinction spectra of gold-nanoparticle arrays with the same periodicity on a thin (30 nm) ITO film (see Fig. 1b, dashed line), since the ITO film supports no waveguide modes in the spectral range of the particle–plasmon resonance.

Further confirmation of the model is provided by experiments on gold-nanoparticle arrays on top of a 140-nm-thick ITO film deposited on a ZnSe substrate. In contrast to the measurements with the quartz substrate, no induced transmission dips within the particle–plasmon resonance can be

✉ Fax: +49-711/689-1010, E-mail: linden@servix.mpi-stuttgart.mpg.de

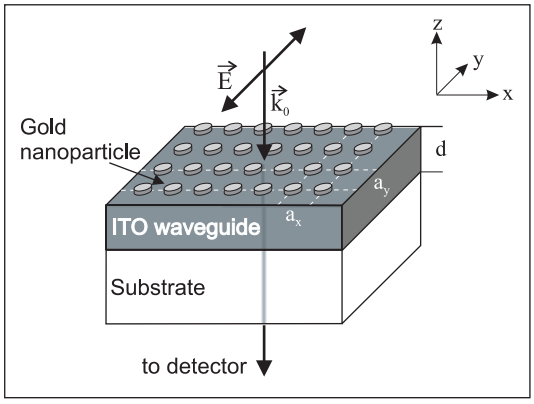

a

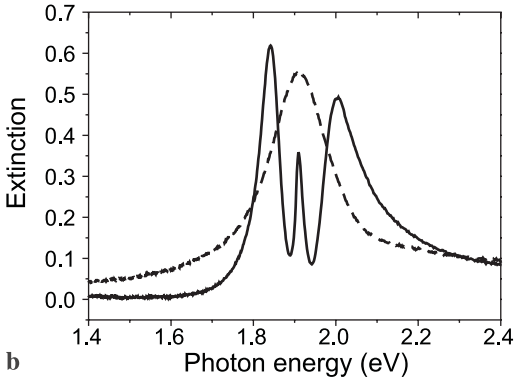

b

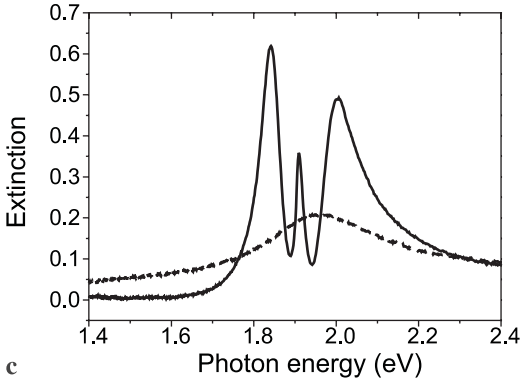

c

FIGURE 1 **a** Sketch of the sample geometry. **b** Extinction of gold nanoparticles arranged with periods of $a_x = 400$ nm along the *x-axis* and $a_y = 300$ nm along the *y-axis*. *Solid line*: quartz-glass substrate covered with a 140-nm-thick ITO film. *Dashed line*: quartz-glass substrate covered with only 30-nm ITO. **c** Extinction of gold nanoparticles arranged with periods $a_x = 400$ nm and $a_y = 300$ nm. *Solid line*: quartz-glass substrate covered with a 140-nm-thick ITO film. *Dashed line*: ZnSe substrate covered with a 140-nm-thick ITO film

observed (see Fig. 1c, dashed line). The reason is the dielectric constant of ZnSe ($\varepsilon_{\mathrm{ZnSe}} = 5.8$), which is larger than the dielectric constant of ITO ($\varepsilon_{\mathrm{ITO}} = 3.8$). Therefore no waveguide mode is supported in the ITO film and photonic interaction between the localized particle plasmons is suppressed.

These findings are very interesting from a fundamental point of view and may also find applications in the design of optical devices. In this paper, we report on the influence of different waveguide modes on the extinction spectrum. Depending on the arrangement of the gold nanoparticles, either transverse electric or transverse magnetic (TM) waveguide modes can be excited for a fixed polarization of the incident light field. This results in a spectral shift of the high-transmission bands for the transition from a TE to a TM waveguide mode in accordance with the calculated dispersion of a slab waveguide.

The samples for our experiments were prepared by electron-beam lithography on quartz-glass substrates covered with a 140-nm-thick ITO film. Two sets of samples were manufactured, arranging the gold nanoparticles in rectangular arrays with periods a_x and a_y along the x-axis and the y-axis (see Fig. 2a), respectively. In order to control the influence of varying sample-preparation conditions during different runs of the lithographic process, we used arrays with a grating constant of 300 nm for both axes as a reference. For the different arrays of the first set, we kept the periodicity along the y-axis fixed at $a_y = 300$ nm while a_x was increased from $a_x = 350$ nm to $a_x = 475$ nm in steps of 25 nm. In the second set, a_x and a_y exchanged their roles. Since the individual particles had a slightly elongated shape with the same orientation for all arrays, the two sets could be distinguished without ambiguity. The diameter of the particles along the x-axis was 120 nm and along the y-axis 100 nm (see Fig. 2a). The height of the gold particles was 20 nm. The lateral extension of the arrays was 100 μm × 100 μm each.

We performed optical transmission experiments for normal incidence with a focused white-light beam in order to determine the extinction ($= -\ln(I_{\mathrm{T}}/I_0)$, I_{T}: transmitted intensity, I_0: incident intensity) of our samples. Due to the elliptical shape of the individual particles, there are two particle–plasmon resonances associated with the two axes for normal incidence [10]. These resonances can be selectively excited by light linearly polarized parallel to the correspond-

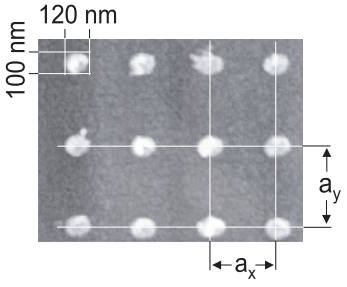

a

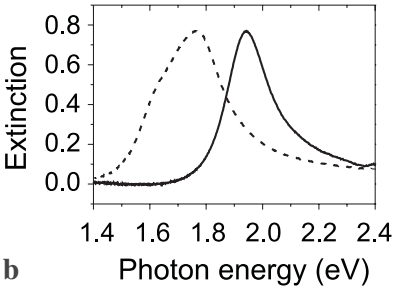

b

FIGURE 2 **a** SEM picture of a gold-nanoparticle array. The gold nanoparticles are arranged with periods a_x and a_y along the *x-axis* and the *y-axis*, respectively. The diameter of the particles along the *x-axis* is 120 nm and along the *y-axis* 100 nm. **b** Extinction of gold nanoparticles on a 140-nm-thick ITO waveguide and periods of 300 nm along both axes. *Solid line*: polarization of incident light field is parallel to *short axis* (*y-axis*) of the nanoparticles. *Dashed line*: polarization of incident light field is parallel to *long axis* (*x-axis*) of the nanoparticles

ing axis (see Fig. 2b). Within the remainder of this paper, all measurements were performed with light polarized parallel to the y-axis in order to exclusively excite the higher-energy particle–plasmon resonance associated with the shorter axis.

The dotted line in Fig. 3a is the extinction spectrum of a reference array ($a_x = a_y = 300\,\text{nm}$) with its particle–plasmon resonance peaked at 1.94 eV and a FWHM of approximately 0.19 eV. The extinction spectra of the first set of samples exhibit new spectral features. For $a_x = 350\,\text{nm}$, two dips with a separation of 0.04 eV appear at 2.11 eV on the high-energy side of the particle–plasmon resonance (Fig. 3a, solid line). Increasing a_x shifts the dips to lower energies and at the same time they become more pronounced (Fig. 3b–d, solid line). When the spectral position of the dips coincides with the peak of the particle–plasmon resonance ($a_x = 400\,\text{nm}$), the extinction in the dips is reduced to $\approx 10\%$ of the extinction of the reference field[1]. For the largest values of a_x, the character of the new feature is changed from induced transmission to enhanced extinction (Fig. 3e–f, solid line).

A similar behavior can be observed for the second set of samples (see Fig. 3, dashed line), when a_y is increased. However, the new spectral features are shifted by approximately 0.18 eV to higher energies compared to the features in the extinction spectra of the corresponding array from the first set of samples.

To explain these experimental results, the model proposed in [8] has to be extended in order to take different waveguide modes into account. Gold nanoparticles are arranged with periods a_x and a_y on top of a quartz-glass substrate (dielectric constant: ε_{Sub}) that is covered with an ITO film of thickness d and dielectric constant ε_{ITO}. The incident light with photon energy $\hbar\omega_0$ has a wave vector $\boldsymbol{k}_0$ and is polarized along the y-axis. Excitation of the particle plasmon associated with the short axis of the gold nanoparticles leads to absorption and scattering of the incident light and is therefore responsible for the spectrally broad extinction spectrum.

Due to the regular two-dimensional arrangement of the gold nanoparticles, it is possible to excite waveguide modes

[1] One has to take into account the geometrical effect that the extinction decreases due to the smaller number of gold nanoparticles per unit area for increasing periods.

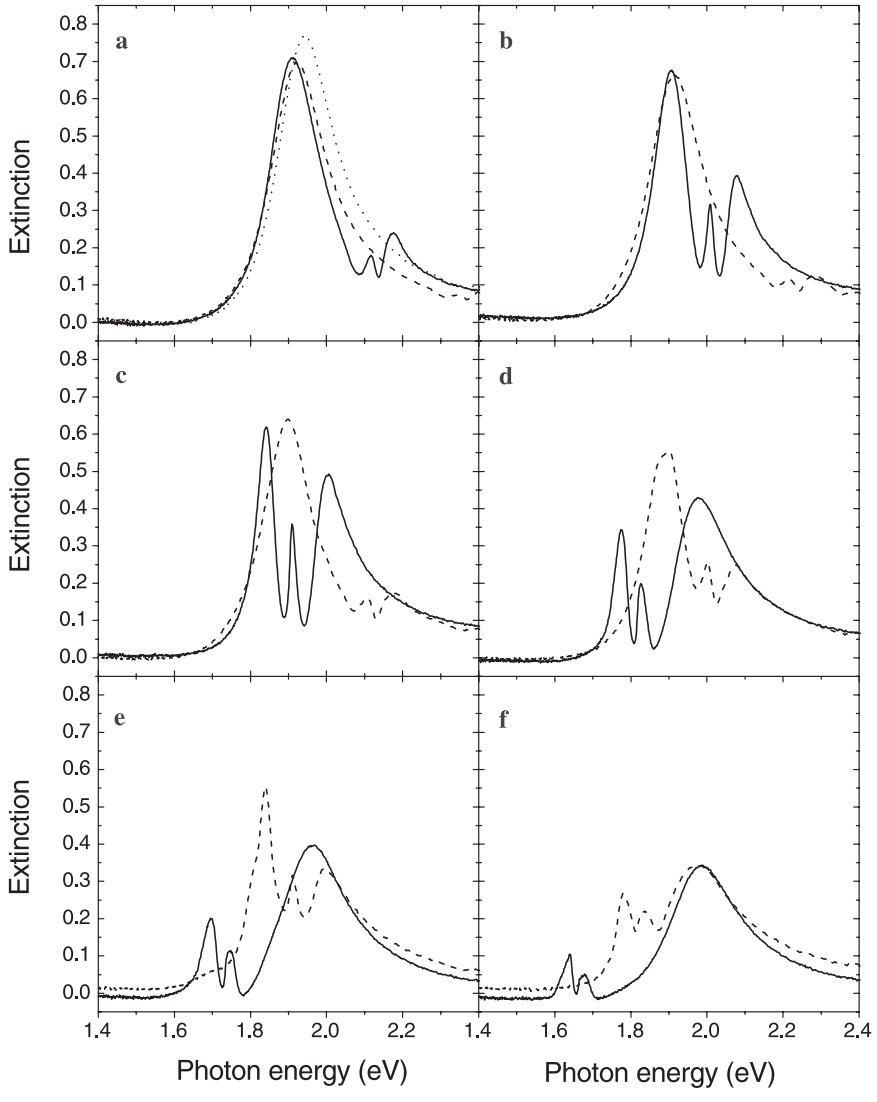

FIGURE 3 Extinction of gold nanoparticles on a 140-nm-thick ITO waveguide for normal incidence. The incident light field is always polarized along the *y-axis*. *Solid line*: first set of arrays – $a_y = 300\,\text{nm}$, $a_x = 350\,\text{nm}$ to $a_x = 475\,\text{nm}$ in steps of 25 nm (**a**–**f**). *Dashed line*: second set of arrays – $a_x = 300\,\text{nm}$, $a_y = 350\,\text{nm}$ to $a_y = 475\,\text{nm}$ in steps of 25 nm (**a**–**f**). *Dotted line* (**a**): reference array with $a_x = a_y = 300\,\text{nm}$

propagating in different directions for frequencies above the cutoff frequency [11]

$$\omega_{\mathrm{cut}} = \frac{c \arctan\left(\sqrt{\frac{\varepsilon_{\mathrm{Sub}}-\varepsilon_{\mathrm{Air}}}{\varepsilon_{\mathrm{ITO}}-\varepsilon_{\mathrm{Sub}}}}\right)}{d\sqrt{\varepsilon_{\mathrm{ITO}}-\varepsilon_{\mathrm{Sub}}}}. \quad (1)$$

For our experimental parameters ($d = 140$ nm, $\varepsilon_{\mathrm{ITO}} = 3.8$, $\varepsilon_{\mathrm{Sub}} = 2.1$, $\varepsilon_{\mathrm{Air}} = 1$; c is the speed of light in vacuum), the corresponding cutoff energy is $\hbar\omega_{\mathrm{cut}} = 0.73$ eV. Efficient coupling from the incident beam to the waveguide requires that the phase-matching condition

$$\boldsymbol{k}_{\mathrm{wg}} = \boldsymbol{k}_{||} \pm i\boldsymbol{g}_x \pm j\boldsymbol{g}_y \quad (2)$$

has to be fulfilled. Here, $\boldsymbol{k}_{\mathrm{wg}}$ is the wave vector of the waveguide mode, $\boldsymbol{k}_{||}$ is the component of the wave vector of the incident light field in the x–y plane, and i and j are integers. $\boldsymbol{g}_x$ and $\boldsymbol{g}_y$ are reciprocal lattice vectors defined by $|\boldsymbol{g}_x| = 2\pi/a_x$ and $|\boldsymbol{g}_y| = 2\pi/a_y$, respectively. We restrict the discussion to ($i = \pm 1$, $j = 0$) or ($i = 0$, $j = \pm 1$) and normal incidence ($\boldsymbol{k}_{||} = 0$), for which only one reciprocal lattice vector is involved in coupling a part of the incident light field into one of the waveguide modes. In this case, the wave vector of a waveguide mode propagating in the x-direction is exclusively determined by a_x, while the wave vector of a waveguide mode propagating in the y-direction only depends on a_y. If the gold nanoparticles had no further influence on the waveguide, one would expect to find in each case two energetically degenerate waveguide modes propagating in opposite directions. However, Bragg scattering of the waveguide modes at the regularly arranged gold nanoparticles leads for both directions to the formation of two standing waves with nodes under and between the gold nanoparticles. The different dielectric environments seen by these different standing waves remove the degeneracy.

Whether light is coupled into a TE or a TM mode for a certain direction depends on the polarization of the incident light field [12]. As a waveguide mode has a distinct polarization (TE or TM), the mode to be excited must have the same polarization as the incident beam (electric field along the y-axis and magnetic field parallel to the x-axis). Under our experimental conditions, a part of the incident radiation is converted by a reciprocal lattice vector g_x into a TE waveguide mode (electric field parallel to the y-axis) propagating along the x-axis (see Fig. 4a). Coupling of light into the waveguide by a reciprocal lattice vector g_y in the y-direction leads to the excitation of a TM waveguide mode (magnetic field parallel to the x-axis) (see Fig. 4b). Both TE and TM waveguide modes are able to interfere with the incident light field. This leads to selective suppression of extinction or additional extinction depending on whether the mode is resonant to the particle plasmon or not. According to these considerations, the additional spectral features in the extinction spectra (see Fig. 3) of the first set (variation of a_x) and the second set of samples (variation of a_y) are caused by excitation of TE and TM waveguide modes, respectively. The spectral features connected with the TM waveguide modes for $a_y = 300$ nm (first set) and the TE waveguide modes for $a_x = 300$ nm (second set) are outside of our observed spectral range.

Figure 5 shows the calculated dispersions [12] of the TE and TM waveguide modes of a simple dielectric slab waveguide (without gold nanoparticles on top) for our experimental parameters. The calculated dispersion curves of both modes start at the same cutoff energy. For photon energies just above this cutoff energy, the TE and TM waveguide modes largely extend into the substrate. Therefore the dispersion relations are asymptotically given by the quartz light line. By increasing the photon energy, the modes become more and more concentrated in the ITO film and the dispersions become more ITO-like. For the same value of $|\boldsymbol{k}_{\mathrm{wg}}|$, the TM waveguide mode has a larger photon energy than the TE waveguide

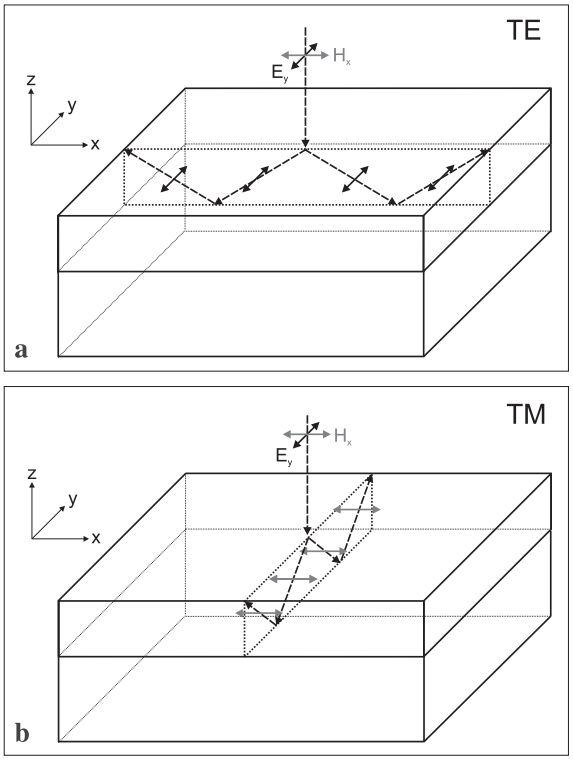

FIGURE 4 Coupling of the incident light field **a** to a TE waveguide mode and **b** to a TM waveguide mode

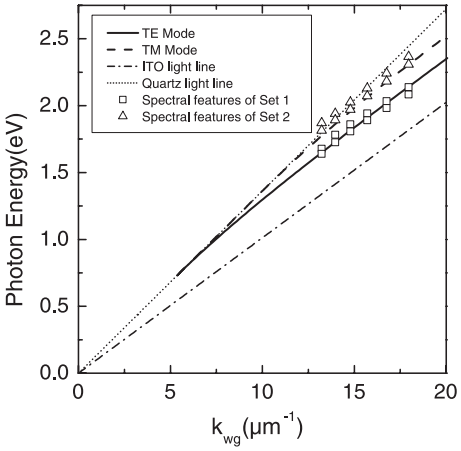

FIGURE 5 Calculated dispersion relations of the TE and TM waveguide modes for an ITO waveguide on quartz glass ($d = 140$ nm, $\varepsilon_{\mathrm{ITO}} = 3.8$, $\varepsilon_{\mathrm{Sub}} = 2.1$, $\varepsilon_{\mathrm{Air}} = 1.0$). The measured values correspond to the additional spectral features (dips within the particle–plasmon resonance, peaks outside the particle–plasmon resonance) in the extinction spectra of Fig. 4

mode. This explains the observed shift to higher photon energies of the additional spectral features in the extinction spectra of the second set of samples compared to the corresponding spectra of the first set. The calculated energy difference is in good agreement with the measured energetic shift (see Fig. 5). Deviations between theory and experiment can be explained by the fact that in the calculated dispersion the presence of the gold nanoparticles is not taken into account and by uncertainties of the exact waveguide parameters.

The influence of different waveguide modes on the extinction spectra of a specific gold-nanoparticle array can also be studied by changing the direction of incidence. As an example, we take an array with periods of $a_x = 400\,\text{nm}$ and $a_y = 300\,\text{nm}$ on a 140-nm-thick ITO waveguide. For normal incidence, the extinction spectrum exhibits two pronounced dips within the particle–plasmon resonance (see Fig. 6, 0°) caused by interference between the incident light field and the excited TE waveguide modes.

By rotating the sample around the y-axis, $\boldsymbol{k}_x$ (component of $\boldsymbol{k}_0$ parallel to the x-axis) can be continuously increased. According to (2), this yields two TE waveguide modes with different absolute values of the wave vector $|\boldsymbol{k}_{\text{wg}}|$ resulting from adding or subtracting a reciprocal lattice vector $\boldsymbol{g}_x$ to or from $\boldsymbol{k}_x$. While the corresponding photon energies are resonant to the particle plasmon (see Fig. 6, dashed line), the two modes manifest themselves as two extinction dips shifting away from each other for increasing angles of incidence. For larger angles, the modes are tuned out of resonance and therefore appear as additional small extinction peaks.

If on the other hand the sample is rotated around the x-axis, $\boldsymbol{k}_y$ (component of $\boldsymbol{k}_0$ parallel to the y-axis) is increased. Since $\boldsymbol{k}_y$ and $\boldsymbol{g}_x$ are perpendicular to each other, the excited waveguide modes will not propagate parallel to the x-axis or the y-axis, but according to (2) in a direction specified by the vectorial sum of $\boldsymbol{k}_y$ and $\boldsymbol{g}_x$. The absolute value of the wave vectors of the waveguide modes is given by $|\boldsymbol{k}_{\text{wg}}| = \sqrt{|\boldsymbol{k}_y|^2 + |\boldsymbol{g}_x|^2}$. This explains the slight shift of both dips to higher photon energies (see Fig. 6, solid line) for increasing rotation angles around the x-axis. An additional dip in the extinction spectra can be observed for angles larger than 15° on the high-energy side of the particle–plasmon resonance. This third dip shifts to smaller photon energies for increasing angles of incidence and results from excitation of a TM waveguide mode. Its wave vector is given by the difference between $\boldsymbol{k}_y$ and the reciprocal

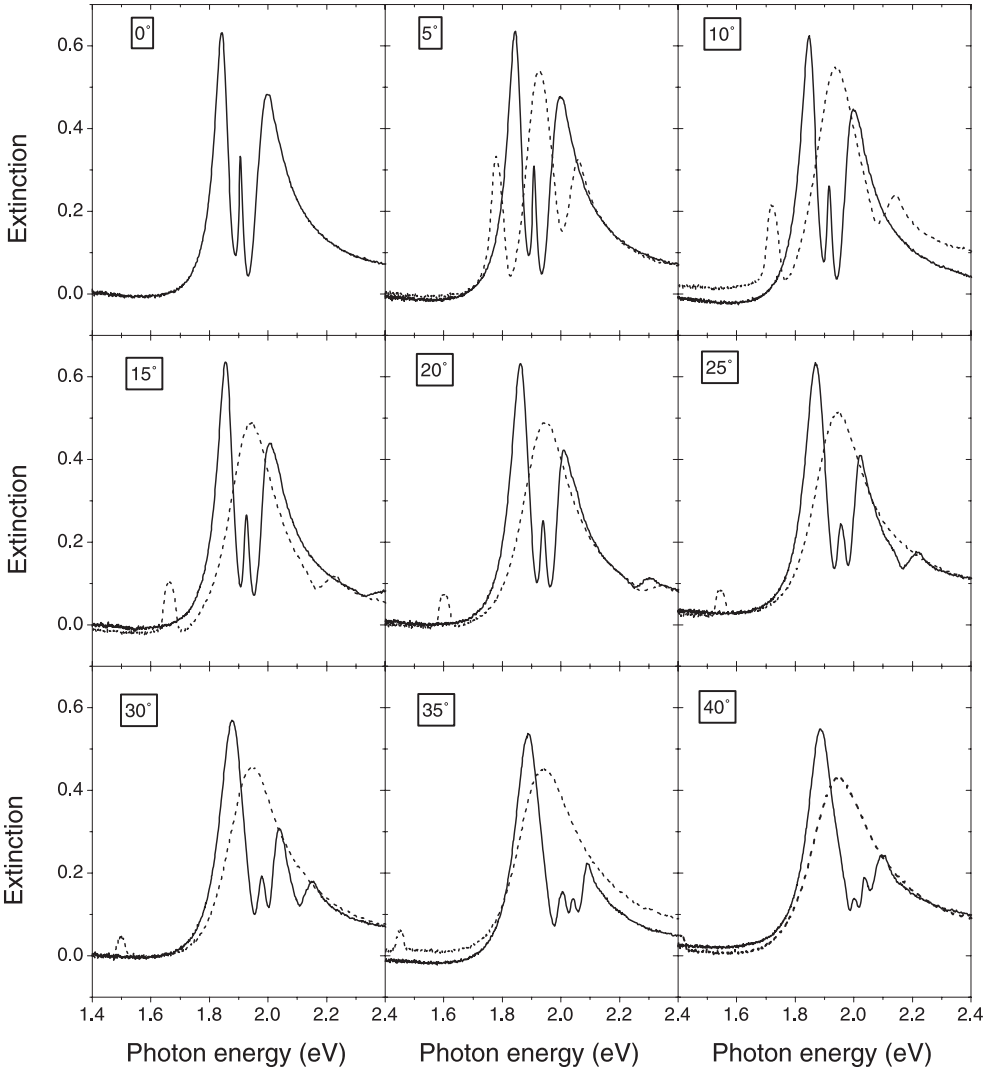

FIGURE 6 Extinction spectra of a gold-nanoparticle array with periods $a_x = 400\,\text{nm}$ and $a_y = 300\,\text{nm}$ on a 140-nm-thick ITO waveguide for different rotation angles around the *y-axis* (*dashed line*) and around the *x-axis* (*solid line*)

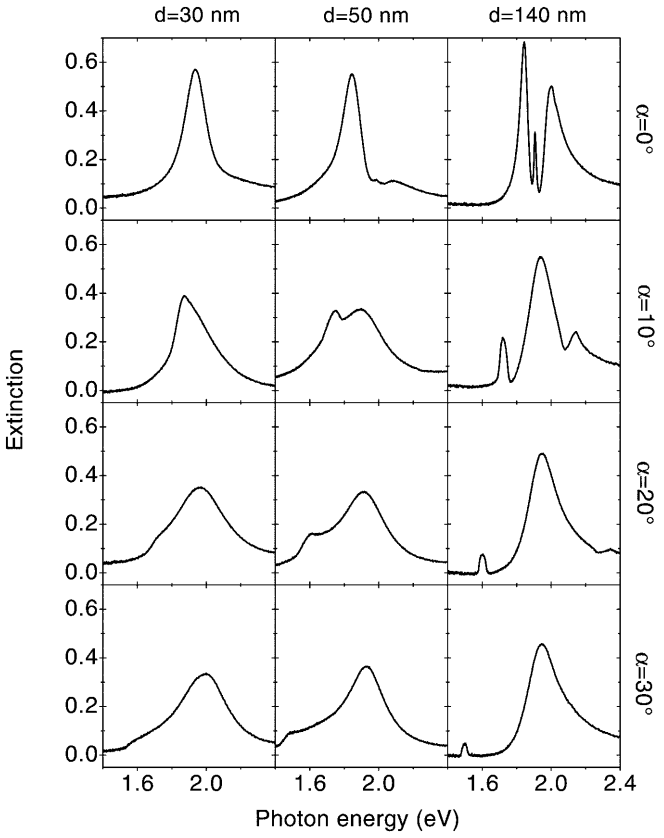

FIGURE 7 Extinction spectra of a gold-nanoparticle array with periods $a_x = 425\,\text{nm}$ and $a_y = 300\,\text{nm}$ on a 30-nm- (*first row*), a 50-nm- (*second row*), and a 140-nm- (*third row*) thick ITO film for different rotation angles around the *y-axis*. The corresponding calculated cuttoff energies are $\hbar\omega_{\text{cut}} = 3.42\,\text{eV}$, $\hbar\omega_{\text{cut}} = 2.05\,\text{eV}$, and $\hbar\omega_{\text{cut}} = 0.73\,\text{eV}$, respectively

lattice vector $\boldsymbol{g}_y$. Note that the second TM waveguide mode cannot be observed, since it is shifted to higher energies even further out of our spectral range.

Starting from the previous experiments, it is interesting to study the influence of the transition from the guiding regime to the non-guiding regime of the ITO film on the extinction spectrum of a gold-nanoparticle array. For this investigation, we have prepared arrays with periods $a_x = 425\,\text{nm}$ and $a_y = 300\,\text{nm}$ on a 30-nm-, a 50-nm-, and a 140-nm-thick ITO film. The corresponding calculated cutoff energies are $\hbar\omega_{\text{cut}} = 3.42\,\text{eV}$, $\hbar\omega_{\text{cut}} = 2.05\,\text{eV}$, and $\hbar\omega_{\text{cut}} = 0.73\,\text{eV}$, respectively. In order to examine the transition, $|\boldsymbol{k}_{\text{wg}}|$ is decreased continuously by rotating the samples around the y-axis by an angle α, so that the corresponding photon energy can be shifted below $\hbar\omega_{\text{cut}}$. The extinction spectra of all three samples for $\alpha = 0°$, $\alpha = 10°$, $\alpha = 20°$, and $\alpha = 30°$ are shown in Fig. 7. The extinction spectra of the nanoparticle array on the 30-nm-thick ITO film (Fig. 7, first column), which supports no guided modes in the spectral region of interest, can be explained with the model of [7]. A strong dipolar interaction of the nanoparticles arises when the light fields corresponding to a particular grating order change from evanescent to radiative character. The critical wavelength at which this transition occurs for the first grating order of the substrate side, normal incidence, and a fixed periodicity a_x, is given by $\lambda_{\text{c}} = a_x\sqrt{\varepsilon_{\text{Sub}}}$. Here, the influence of the thin ITO film is neglected. The corresponding photon energy for our experimental conditions ($a_x = 425\,\text{nm}$, $\varepsilon_{\text{Sub}} = 2.1$) is $\hbar\omega_{\text{c}} = 2.01\,\text{eV}$. For photon energies above this critical value, the radiative grating order causes an additional radiative damping of the particle plasmon. By rotating the sample, $\hbar\omega_{\text{c}}$ is decreased, which results in an enhanced extinction on the low-energy side of the particle–plasmon resonance (Fig. 7, first column, $\alpha = 20°$ and $\alpha = 30°$). The extinction spectrum of the gold-nanoparticle array on the 50-nm-thick ITO film exhibits two dips for normal incidence (Fig. 7, second column, $\alpha = 0°$). Therefore, we conclude that there still exists a guided mode, even if the dips appear slightly below the calculated cutoff energy. This can most likely be explained by deviations from the nominal parameters. For $\alpha = 30°$ (Fig. 7, second column, $\alpha = 30°$), the features of a guided mode disappear. Instead, a shoulder on the low-energy side of the particle–plasmon resonance can be observed as for the sample on the 30-nm-thick ITO film. This is a strong indication that there exists no guided mode any more and we observed the transition from the guiding to the non-guiding regime of the ITO film. In contrast, the 140-nm-thick ITO film (Fig. 7, third column) allows the excitation of waveguide modes for the whole observed spectral range, and we again observe the results from the previous experiment.

In conclusion, we have presented optical transmission measurements on regular gold-nanoparticle arrays deposited on top of a dielectric waveguide. The spectra exhibit spectrally narrow bands of suppressed extinction within the particle–plasmon resonance resulting from destructive interference between the incident light field and excited waveguide modes. The influence of TE and TM waveguide modes on the extinction spectrum has been investigated by variation of the chosen arrangement of the gold nanoparticles for a fixed polarization of the incident light field. The observed spectral shift of the high-transmission bands for the transition from a TE to a TM waveguide mode is in good agreement with the calculated dispersion for a slab waveguide.

ACKNOWLEDGEMENTS We thank W. Rühle and K. von Klitzing for continuous support and U. Schröter, M. Totzeck, and F.J. Garcia-Vidal for stimulating discussions.

REFERENCES

1 U. Kreibig, M. Vollmer: *Optical Properties of Metal Clusters* (Springer, Berlin 1995)
2 G. Mie: Ann. Phys. **25**, 377 (1905)
3 H. Wetzel, H. Gerischer: Chem. Phys. Lett. **76**, 460 (1980)
4 D. Ricard, Ph. Roussignol, Chr. Flytzanis: Opt. Lett. **10**, 511 (1985)
5 H.G. Craighead, G.A. Niklasson: Appl. Phys. Lett. **44**, 1134 (1984)
6 W. Gotschy, K. Vonmetz, A. Leitner, F.R. Aussenegg: Appl. Phys. B **63**, 381 (1996)
7 B. Lamprecht, G. Schider, R.T. Lechner, H. Ditlbacher, J.R. Krenn, A. Leitner, F.R. Aussenegg: Phys. Rev. Lett. **84**, 4721 (2000)
8 S. Linden, J. Kuhl, H. Giessen: Phys. Rev. Lett. **86**, 4688 (2001)
9 S. Herminghaus, M. Klopfleisch, H.J. Schmidt: Opt. Lett. **19**, 293 (1994)
10 R.J. Warmack, S.L. Humphrey: Phys. Rev. B **34**, 2246 (1986)
11 H. Kogelnik, V. Ramaswamy: Appl. Opt. **13**, 1857 (1974)
12 P.K. Tien, R. Ulrich, R.J. Martin: Appl. Phys. Lett. **14**, 291 (1969)